Electrochemical Fabrication of Surface Chemical Gradients in Thiol Self-Assembled Mono layers with Tailored Work-Functions

ARTICLE *in* LANGMUIR · SEPTEMBER 2014

Impact Factor: 4.46 · DOI: 10.1021/la5013928 · Source: PubMed

Langmuir

Article

pubs.acs.org/Langmuir

Electrochemical Fabrication of Surface Chemical Gradients in Thiol Self-Assembled Monolayers with Tailored Work-Functions

Giulia Fioravanti,*[,†] Francesca Lugli,[§] Denis Gentili,[‡] Vittoria Mucciante,[†] Francesca Leonardi,[‡] Luca Pasquali,[∥,#,∇] Andrea Liscio,[⊥] Mauro Murgia,[‡] Francesco Zerbetto,[§] and Massimiliano Cavallini*[,‡]

[†]Dipartimento di Scienze Fisiche e Chimiche, Università dell'Aquila, Via Vetoio 1, 67100 L'Aquila, Italy

[§]Dipartimento di "Chimica G. Ciamician", Università di Bologna, V. F. Selmi 2, 40126 Bologna, Italy

[‡]Istituto per lo Studio dei Materiali Nanostrutturati (ISMN) and [⊥]Istituto per la Sintesi Organica e la Fotoreattività (ISOF), Consiglio Nazionale delle Ricerche (CNR), Via P. Gobetti 101, 40129 Bologna, Italy

[∥]Dipartimento di Ingegneria "Enzo Ferrari", Università di Modena e Reggio Emilia, Via Vignolese 905, 41125 Modena, Italy

[#]CNR - Istituto Officina dei Materiali, S.S. 14, km 163.5 in Area Science Park, I-34012 Trieste, Italy

[∇]Department of Physics, University of Johannesburg, PO Box 524, Auckland Park, 2006, South Africa

Supporting Information

ABSTRACT: The studies on surface chemical gradients are constantly gaining interest both for fundamental studies and for technological implications in materials science, nanofluidics, dewetting, and biological systems. Here we report on a new approach that is very simple and very efficient, to fabricate surface chemical gradients of alkanethiols, which combines electrochemical desorption/partial readsorption, with the withdrawal of the surface from the solution. The gradient is then stabilized by adding a complementary thiol terminated with a hydroxyl group with a chain length comparable to desorbed thiols. This procedure allows us to fabricate a chemical gradient of the wetting properties and the substrate work-function along a few centimeters with a gradient slope higher than 5°/cm. Samples were characterized by cyclic voltammetry during desorption, static contact angle, XPS analysis, and Kelvin probe. Computer simulations based on the Dissipative Particle Dynamics methods were carried out considering a water droplet on a mixed SAM surface. The results help to rationalize the composition of the chemical gradient at different position on the Au surface.

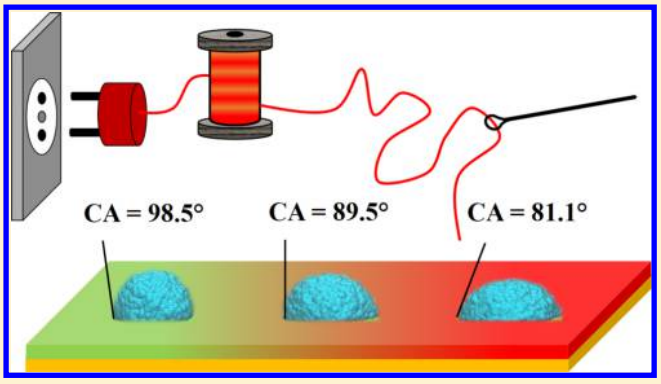

INTRODUCTION

Surface chemical gradients are the focus of growing interest both in terms of fundamental studies and for technological implications in materials science,[1] nanofluidics,[2−6] technological application of dewetting,[7] and biological systems.[8,9]

Several methods have been proposed for the fabrication of chemical gradients on a solid substrate. They include chemical vapor deposition,[10−13] solution controlled deposition,[14−17] contact printing,[18−20] photoirradiation,[21−23] photodegradation,[24,25] thermal treatment,[26] and others. Many of these techniques are based on the surface modification/deposition of a self-assembled monolayers (SAMs) adsorbed on a substrate.[27,28] Usually these methods include an initially controlled gradual immersion (or extraction) of the surface into (from) a solution containing the molecules able to form the SAM. The result is a surface that features a chemical gradient consisting of an incomplete monolayer in which the coverage is tuned by the dipping time of the surface in the solution. Incomplete SAMs are usually not very stable and tend to reorganize over time. In order to stabilize the incomplete SAM, samples are filled by a second complementary SAM obtained by immersing the surface into a solution with a second complementary molecule, which favors the formation of a stable high density SAM. Unlike many studies that report the formation of a binary monolayer coating,[29,30] derived from the coadsorption of two different species without precise control over the composition, the formation of a surface chemical gradient could be obtained with extreme accuracy.

Currently, efforts are directed toward the control of the directionality and the chemical composition of the gradients obtained by using two different species, through a controlled assembly (from the liquid phase[6,10,15,17]) or by post-treatment of the monolayer via an external stimulus (thermal,[11,26] radiative,[24,31] etc.). Varying the composition of binary hydrophilic−hydrophobic SAMs allows tailoring of the wetting properties of a surface in a continuous manner. This property

Received: April 10, 2014
Revised: September 10, 2014
Published: September 15, 2014

has been exploited to generate smart materials and to investigate surface-driven transport phenomena such as the motion of water droplets on a wettability gradient[2,3,6,12,32] and the study of biological processes such as the selective adhesion and growth of cells/proteins on gradients.[8,9]

Two highly used types of SAMs are alkyl silanes on oxide surfaces[33] and sulfur-containing molecules on gold. Because of their ease of preparation, the spontaneous formation of a densely packed monolayer, and the conductivity of the substrate, the assembly of ω-functionalized thiols on gold has been extensively studied, including the application to surface chemical gradient formation.[34,35]

A major advancement in surface chemical gradients (SCG) fabrication has been provided by electrochemical methods, which take advantage of the fine-tuning of monolayer adsorption/desorption by the electrode potential,[36] allowing high control of the SAM composition and the fabrication of higher gradients. Several papers reported the electrochemical method for the assisted preparation of monolayers and bilayers of several kinds of thiols by controlling the electrode potential in the presence of reagents in solution.[37,38]

Phase-segregated binary SAMs were achieved first by preparing a full monolayer of the first thiol, then oxidative/reductive desorption was carried out using electrochemical protocols to remove a fraction of the original SAM.[39−42] Once desorption has taken place, the vacancies created could be filled by exposure to a solution with a second thiol. This procedure is very efficient but does not provide spatial control of the chemical composition of the monolayer; it leads to separated phases of binary self-assembled thiols, without a chemical gradient.[41,43,44]

The controlled desorption of thiol monolayers by electrochemical control has been used to obtain single component chemical gradients. In particular, the reductive desorption/partial readsorption of thiols SAM on noble metal surfaces was exploited, followed by a backfilling step to gain binary gradient SAM. Terrill et al. presented a method that relies on the electrochemical desorption of alkanethiols from a fully covered SAM by application of a potential in a flow-cell.[45] Bohn et al. obtained a gradient of thiols exploiting a linear potential variation with position along a gold surface, by poising the two ends of a thin Au strip at different potentials relative to a common solution Ag/AgCl reference couple.[46]

Here we report on a new method to fabricate a SCG of alkanethiols, which combines the reductive electrochemical desorption/partial readsorption of thiols, performed by cycling the electrode potential, while the surface is withdrawn from the solution. The gradient is then stabilized by adding a complementary thiol characterized by the same chain length, in order to stabilize the SAM, but with a different end group (e.g., −OH vs $-CH_3$). We fabricate a chemical gradient of the wetting properties and the substrate work-function along a few centimeters with a gradient slope higher than 5°/cm. Samples were characterized by contact angle (static experiments), XPS analysis, Kelvin Probe (KP), and electrochemical techniques. Computer simulations based on the Dissipative Particle Dynamics (DPD) methods were carried out considering a water droplet on a mixed SAM surface. The results help to rationalize the composition of the chemical gradient at different position on the Au surface.

EXPERIMENTAL SECTION

Materials. A polycrystalline Au coated glass substrate was used as the working electrode. It was prepared by vacuum evaporating 100-nm-thick Au on a 6-nm-thick chromium layer (as adhesive layer). The wafers were cut into samples of ∼1.0 cm × 3.0 cm, for experiments.

Dodecanthiol (DT, C12H26S), 11-mercapto-1-undecanol (MU, C11H24OS), ethanol, potassium hydroxide were obtained from Sigma-Aldrich and used without further purification.

Preparation of SAMs. The Au electrode was first cleaned in freshly prepared piranha solution (3:1 sulfuric acid:hydrogen peroxide) at 100 °C for 5 min, and then quenched with Milli-Q water several times. The complete monolayer of dodecanthiol (DT) was formed on the clean Au surface by the incubation in a freshly prepared 1 mM ethanolic solution for 6 h. The surface was assembled to an alligator clip (contact resistance <10 Ω), and connected to a potentiostat (Autolab Ecochemie Model PGSTAT20). We use a three-electrode cell, with a reference electrode (Ag/AgCl), a platinum wire as auxiliary electrode, and the gold surface as the working electrode. The reductive desorption/partial readsorption was carried out in 0.5 M KOH solutions in ultrapure water, as electrolyte. After removal from the thiol solution, the surface was rinsed thoroughly with EtOH, to remove any weakly physisorbed thiols. Then the substrate was sonicated in acetone, isopropanol, and water and dried under nitrogen. After the desorption/partial readsorption step the surface was immersed in a diluted 0.5 mM solution of 11-mercapto-1-undecanol (MU) in ethanol for 12 h, then rinsed with EtOH and H_2O, and dried under nitrogen.

Techniques. The static water contact angles (CA) were measured at 25 °C in air using a contact angle meter (GBX Digidrop instrument) using sessile drop method. Each experimental point reported in the graphs was determined as the average value measured at the least three times for each point. The experiments were reproduced in more than 10 samples for each gradient. The volume of the deionized (DI) water used for these measurements was 1 μL in accordance with the volume used in the simulation.

Macroscopic Kelvin Probe measurements were performed under ambient conditions using 2-mm-diameter gold tip amplifier (Ambient Kelvin Probe Package from KP Technology Ltd.). The technique provides a voltage resolution of about 5 mV. Calibration of the probe was performed using a freshly prepared gold surface. A comprehensive description of the technique can be found in Baikie et al.[47] and references therein. XPS was taken with a double pass cylindrical mirror analyzer (PHI-PerkinElmer model 15-255G) driven at constant pass energy of 50 eV. A dual anode nonmonochromatic X-ray source was used, delivering Mg Kα photons (operated at 15 kV, 15 mA).

RESULTS AND DISCUSSION

Spatially Controlled Electrochemical Desorption. In the experiments, we used a modified emersion method that was originally developed to adsorb in controlled manner SAMs on gold[15,17] using the system schematized in Figure 1 and detailed described in the Supporting Information. The emersion of the substrates was controlled by a computer-driven linear-motion drive, with a speed of 50 μm/s.

The SCG is obtained by withdrawing the surface covered by with a DC SAM while performing a CV from −0.4 to −1.4 V, which induces a reductive desorption/partial readsorption. CV measurements were carried out with an Autolab Ecochemie PGSTAT20 model. As electrolytic solution, we used a 0.5 M KOH solutions in ultrapure water. Immediately after immersing the surface in the solution, the motor started withdrawing the substrate from the solution at a constant rate while the potential of the surface was cycled in the range of −0.4 to −1.4 V. At the end of the process the surface was washed with ethanol and water, and dried under nitrogen. The experiment takes no longer than 10 min and can be done under nitrogen atmosphere.

dx.doi.org/10.1021/la5013928 | Langmuir 2014, 30, 11591−11598

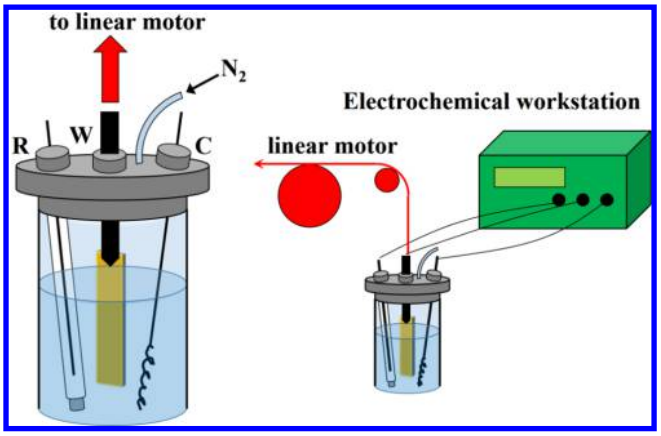

Figure 1. Apparatus for spatially controlled electrochemical desorption. R = Reference electrode (Ag/AgCl); C = Counter electrode (Pt wire); W = Working electrode (Au/SAM platelet).

As reported in the literature, the extent of desorption of the SAM depends on of the applied potential and chain length of the assembled thiols.[42,48,49] We compared our systems with gradients made by holding the potential at a fixed value, while withdrawing the surface, but in this case, the gradient obtained was poorly reproducible and the variability of the CA is as large as the gradient (therefore not experimentally significant). This behavior is probably because, at fixed potential, the system undergoes a more effective desorption, which leads to a partially desorbed monolayer, without a net direction of the gradient. The samples show quasi-constant CA values along the surface, in the length scale of the contact angle measurements considered. Instead, in our case, the gradient obtained by cycling during the sample extraction results in higher slope, much more stable and reproducible. We speculate that this behavior is probably due to the desorption/partial readsorption of the SAM, and therefore to the ability of thiols to reorganize themselves on the surface.

Cyclic Voltammetry on Au/SAM. As previously described in the literature,[38,39,41,43,45] cyclic voltammetry (CV) was used to characterize the presence of thiol monolayers on the gold surface and to further desorption/partial readsorption.

We performed CV at speed of 100 mV/s, in 0.5 M KOH. All potentials are referred to Ag/AgCl reference electrode, and the Au/SAM substrate served as the working electrode. The substrate was contacted using a clip and immersed vertically in the electrolyte solution without wetting the clip (see Figure 1). Figure 2 shows the typical CV of the DT SAM compared to bare surfaces in the negative potential region (at a scan rate of 100 mV/s). This CV was taken under static conditions, where the substrate is not being removed from the electrolyte solution. Initially, in the forward scan, the current is very low (<10 μA/cm^2) as the presence of a SAM reduces the capacitive currents (background current). At about −0.9 V, the current begins to increase due to the onset of reductive desorption (see Figure 2).

As the thiols begin to desorb, there is a pronounced increase in the current due to the desorption process, and the small peak at about −1.25 V corresponds to the point where the SAM begins to desorb. In the subsequent backward scan, a small peak is visible with a maximum at −1.15 V, and is attributed to partial readsorption. The reduction process, with a potential peak at −1.25 V, is characterized by an i_{pc}/i_{pa} ratio slightly higher than unity, suggesting the occurrence of an irreversible

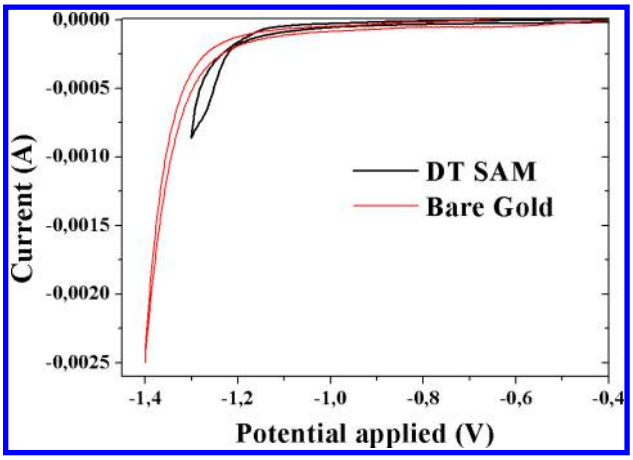

Figure 2. Cyclic voltammetry of bare gold and thiol modified Au surface. Reference electrode: Ag/AgCl; Counter electrode: Pt wire; Working electrode: Au, Au/SAM. Solution: 0.5 M potassium hydroxide (KOH); Speed = 100 mV/s.

reduction reaction. The irreversible reduction, with E_p = −1.25 V, is attributed to Au−S bond cleavage following the process: Au−S−R + e$^-$ → Au + R−S$^-$.

A minor contribution of water electrolysis was observed at the corresponding thiol desorption potential, as shown in Figure 2, where we reported the CV of bare gold electrode.

Withdrawing Electrochemical Desorption. To form the gradient, the electrochemical desorption of DT-SAM was performed combining CV, cycling from a voltage of −0.40 to −1.40 V, with mechanical withdrawal from the solution (Figure 1). Cyclic voltammetry was performed in the conditions established in the previous section (viz. of 100 mV/s, in 0.5 M KOH solutions, cycling from a voltage of −0.40 to −1.40 V. While performing the electrochemical desorption, the gold surface was withdrawn from the liquid, with a constant rate of 50 μm/s. Figure 3 shows the evolution of the CVs during the desorption/partial readsorption.

After the completion of the gradient formation process, the surface was washed with ultrapure water, sonicated in acetone, isopropanol, and water, and dried with nitrogen. Contact angle measurements confirm the presence of a wettability gradient along the length of the surface (see Figure 4, Single SAM plot).

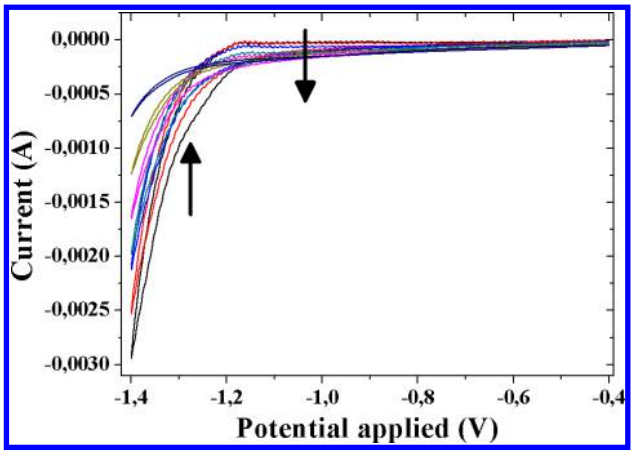

Figure 3. Evolution of CV during the withdrawing combined with electrochemical desorption. A figure containing more CVs is reported in Supporting Information.

dx.doi.org/10.1021/la5013928 | Langmuir 2014, 30, 11591−11598

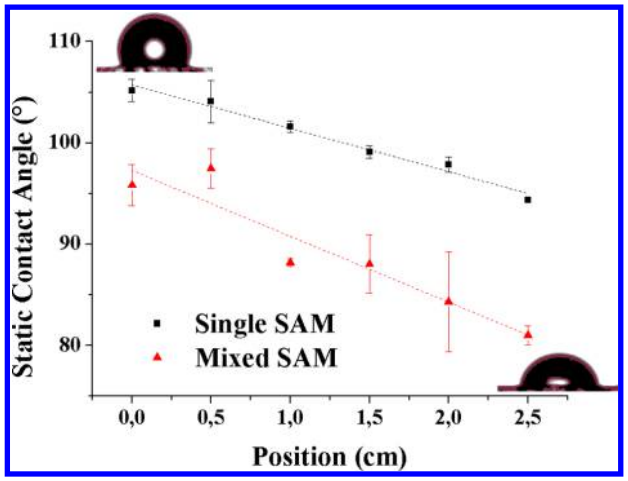

Figure 4. Chemical gradient characterization by water static contact angle.

As expected, the zones of the surface extracted at the beginning of the process (nearest to the clip) show a densely packed SAM, whose contact angle (105°) is comparable with a complete DT monolayer, while the zones at the end of the sample exposed to longer desorption shows a low coverage of the surface which results in a CA closer to bare Au (contact angle ≃85°). The CA for a complete monolayer of 11-mercapto-1-undecanol (MU) is approximately 60°.

The single DT-SAM gradient was then saturated with a complementary thiol 11-mercapto-1-undecanol (MU), and CA measurements were repeated. Figure 4 shows the gradient of static contact angle of single DT-SAM and DT-MU mixed SAM. The gradients trend can fit to a linear equation, represented by the two dotted lines in Figure 4, which correspond to the equations

$$y = 97.3(\pm 1.7) - 6.5(\pm 1.1)x \qquad \text{for Mixed SAM} \tag{1}$$

$$y = 105.7(\pm 0.5) - 4.3(\pm 0.3)x \qquad \text{for Single SAM} \tag{2}$$

Both systems exhibit a linear decrease of about 5°/cm. The addition of MU-SAM shifts the curve toward a more hydrophilic surface, preserving the mean value of the gradient. During the incubation period (12 h) in the MU solution a partial exchange of thiols on the surface occurs; however, this partial exchange does not compromise our aim that was to obtain a stable chemical gradient. Our protocol is permitted because of the higher stability of the DT-SAM, in comparison to the MU-SAM. Noticeably, while single DT-SAM gradient is stable for less than a couple of weeks, mixed DT-MU SAM is stable for more than 1 month. The increased stability is probably due to the formation of a complete monolayer on the surface, which stabilizes the system.

CA measurement shows a higher variability in the first part of the gradient if compared with second part. We speculate that this effect is due to thiol desorption and SAM rearrangement, which is not perfectly uniform at the scale of droplet size (typically <1.4 mm diameter, measured at the beginning of the gradient).

XPS Measurements. To further investigate the formation of a graded surface composition of the DT-SAM, we studied by XPS the variation of the concentration of specific elemental species characteristic of the organic film in different areas of the surface. In particular, we focused on sulfur, which is specific for thiols, through investigation of the intensity of S 2p core levels.

The spectra of the S 2p core levels (Figure 5) show a progressive sulfur reduction when acquisition is carried out on

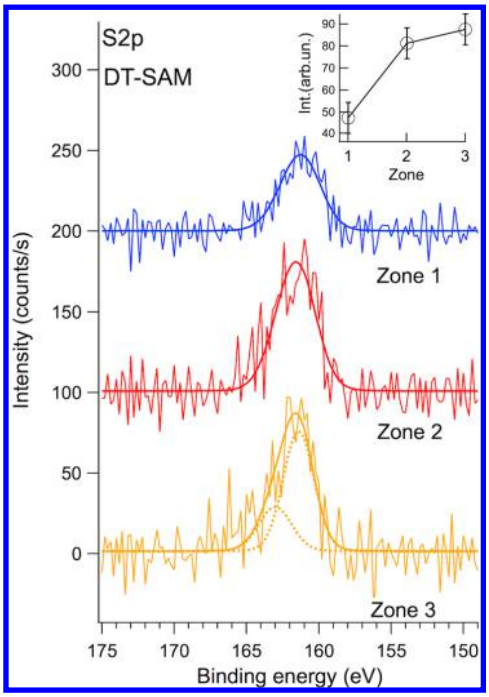

Figure 5. XPS spectra of S 2p core levels taken on different zones of an alkanethiol-graded film on Au. Zone 3 refers to the nondesorbed dodecanthiol film; zone 2 and zone 1 to progressive desorption regions.

differently desorbed areas (from zone 3 to 1 in the order), as emphasized in the inset of the figure where the trend of the peak intensity is presented. This is interpreted in terms of the gradient of molecular concentration at the surface. The peaks were fitted with Voigt doublets, corresponding to the spin-orbit $2p_{3/2}$–$2p_{1/2}$ split components, separated by 1.2 eV. The decomposition into individual peaks is shown, as an example, for zone 3 in Figure 5. The same experimental broadening was assumed for all spectra. The S $2p_{3/2}$ peak position (161.6 eV for zone 3 and 2) is consistent with thiolate species (S–Au bonding). No indication of unbound S or multilayer formation is observed: in these cases a new doublet structure is expected to show up at higher binding energy (163–164 eV), which is not present. A small shift toward lower binding energy is instead observed for the S 2p structure in zone 1 (at 161.2 eV), where the film is supposed to be totally desorbed. In this sense, the binding energy shift is compatible with dissociated S from desorbed molecules, which remains at the surface and is bonded to Au.[50]

Kelvin Probe. The variation of the surface wettability due to the SAM formation reflects on the shift of the contact potential with respect to the bare gold surface. The corresponding contact potential difference (CPD) is given by the effective molecular dipole perpendicular to the substrate, taking into account the depolarization effects due to molecular coverage.[51] For this reason, the SAM formation on the surfaces was monitored by Kelvin Probe by measuring the CPD for different position of the sample as shown in Figure 6 for both single (black square) and mixed SAM (red circles) gradients.

dx.doi.org/10.1021/la5013928 | Langmuir 2014, 30, 11591–11598

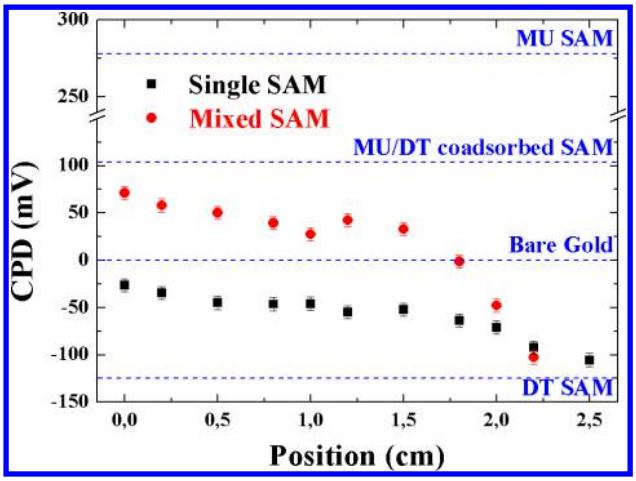

Figure 6. Contact potential difference (CPD) values vs sample distance measured on single (black squares) and mixed SAM (red circles) gradients. CPD values of reference samples without gradient are represented with dashed blue lines.

The distance is given from the final part of the sample, which has mostly remained in solution and should mainly correspond to gold (MU SAM) for single (mixed) SAM gradient. All the CPD values are referred to the potential measured on bare gold (i.e., CPD_{Au} = 0 V). We also measured the potentials of SAM deposited without carrying out the gradient fabrication procedure for single (MU, DT) and mixed (MU/DT coadsorbed) thiols.

Those samples were prepared by simple immersion of the substrate in a diluted ethanol solution of 1-dodecanthiol (DT), thiol 11-mercapto-1-undecanol (MU), and a mixture 1:1 of 1-dodecanthiol and 11-mercapto-1-undecanol (MU/DT coadsorbed). In these cases, the potential does not depend on the position and the values are displayed as horizontal dotted lines. Single and mixed gradient SAMs show different trends that are quite linear in the first case and sigmoidal in the other with a wider variation range, in agreement with the results obtained from the contact angle analysis.

In particular, the measured CPD of single SAM tends to be very close to value measured on gold. It is noteworthy to point out that gold surface in air is contaminated in a few minutes with a change in the corresponding contact potential (a.k.a. work function) of hundreds of mV.[52] Such behavior suggests that the single SAM has undergone a partial desorption, producing different vacations in the SAM and thereby leading to a disordered film. Being not uniform, the film shows patches with different packing and different surface density of thiols. In this case, the isolated alkyl chains are not perpendicular and can lie on the gold surface.

Computer Simulations. Dissipative particle dynamics (DPD) simulations[53−55] were carried out to study the equilibrium contact angle of a water droplet on a functionalized surface as a function of the SAM composition. DPD method is an effective approach to the study of hydrodynamic behavior on a mesoscopic scale and it has been already applied in the simulation of droplets on solid surfaces[56] or under the effect of a shear field.[57] Here the system consists of three phases: two immiscible fluids (the liquid droplet and the vapor) and a solid, which represents the mixed SAM surface of the experiments. The solid phase is modeled by freezing the motion of particles located at the bottom part of a cubic simulation box. In order to represent the different hydrophobic/hydrophilic natures of the different regions of the mixed SAM surface, a random distribution of two different surface beads (see green and red beads in Figure 7) were created on a surface area of 2.5 × 2.5 mm^2.

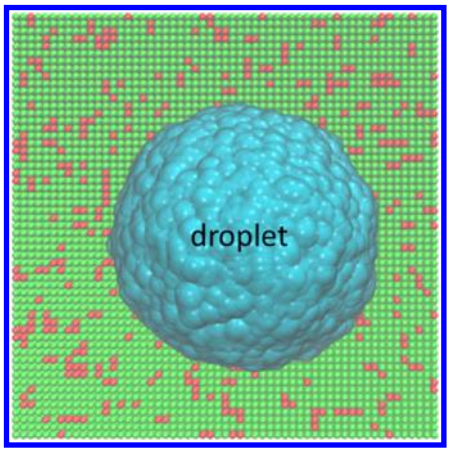

Figure 7. Snapshot of simulation. A water droplet of 1 μL is placed on a mixed SAM square surface (2.5 mm size). Green and red beads represent $-CH_3$ and $-OH$ terminated regions, respectively.

The composition of the mixed SAM can be expressed in terms of hydrophobic ($-CH_3$)/hydrophilic ($-OH$) fractional area, $f_{CH3} = 1 - f_{OH}$. A spherical droplet of radius 0.6 mm (corresponding to 1 μL volume) is initially placed on the surface. At the end of DPD simulation, the equilibrium contact angle is calculated and averaged over the whole trajectory.

In Figure 8, the equilibrium contact angle is plotted as a function of the hydrophobic fractional area f_{CH3}. The values at

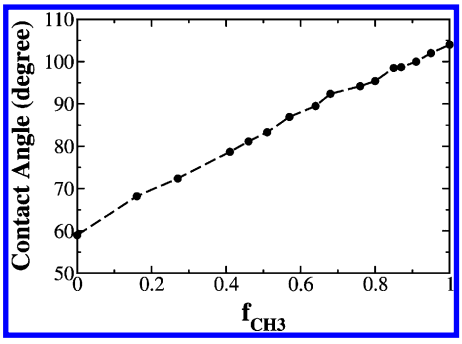

Figure 8. Calculated equilibrium contact angle of a water droplet on a mixed SAM as a function of CH_3 fractional area (f_{CH3}).

the extremes of the plot, $f_{CH3} = 1$ and $f_{CH3} = 0$, reproduce the experimental contact angles of water droplet on a homogeneous single SAM of dodecanthiol ($\theta_{CH3} \approx 104°$) and 11-mercapto-1-undecanol ($\theta_{OH} \approx 60°$), respectively. For a mixed SAM surface Cassie's law, which describes the effective contact angle for a liquid on a composite surface, reads

$$\cos\theta = f_{CH3}\cos\theta_{CH3} + f_{OH}\cos\theta_{OH} \quad (3)$$

Using eq 3 and the measured contact angles, it is possible to estimate the composition of the mixed SAM at different position of the sample (see Figure 9a). The calculated trend reproduces well the results obtained in Kelvin Probe experiments. Along the x direction of the sample, the droplet experiences a sigmoidal gradient. We performed DPD simulations of water droplet dynamics on mixed SAM surfaces,

dx.doi.org/10.1021/la5013928 | Langmuir 2014, 30, 11591−11598

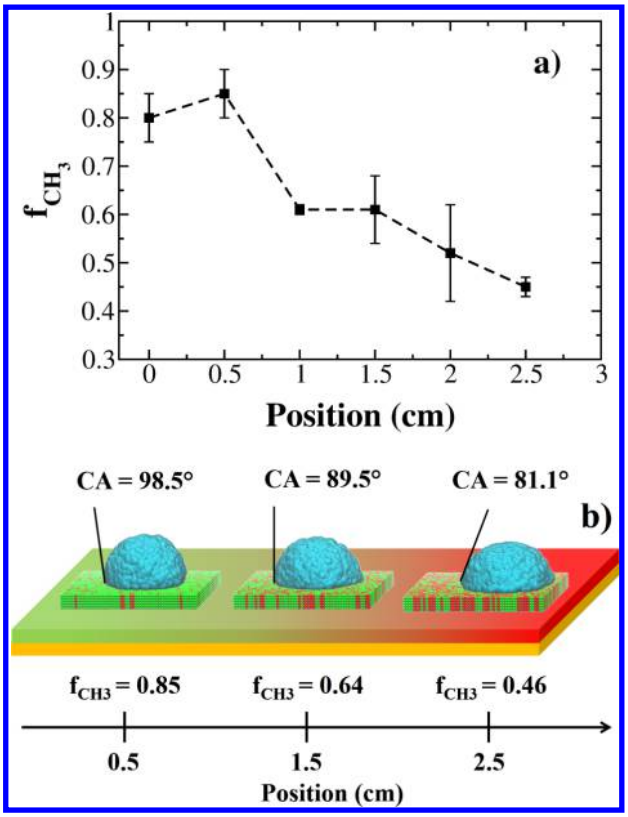

Figure 9. (a) Calculated hydrophobic fractional area f_{CH3} as a function of sample distance for the mixed SAM surface. (b) Snapshots from DPD simulations of water droplet at three different distances (0.5, 1.5, and 2.5 cm) of the sample.

for the six different CH_3 fractional area displayed in Figure 9a. The calculated contact angles reproduce the measured static contact angles of Figure 4. In Figure 9b, three snapshots at three different distances (0.5, 1.5, and 2.5 cm) of the sample are shown.

CONCLUSIONS

In this work, we propose a method to fabricate a reproducible chemical gradient on surfaces combining electrochemical desorption/partial readsorption and extraction from solution of thiols. The combination of these two procedures affords a fine control of the gradient formation that can be increased (or decreased) with respect to conventional approaches that are based on the control of a single parameter (e.g., extraction rate of potential of desorption). In order to prove the efficient gradient formation, samples were characterized by contact angle, XPS, Kelvin Probe, and electrochemical techniques. The results demonstrate that our approach allows us to fabricate a chemical gradient by a simple and fast technique. Furthermore, we have shown the tailoring of the work-function of Au, which is relevant for application of mixed SAMs in organic electronics and photovoltaics. Mesoscopic calculations analyzed in terms of Cassie's law allow determining the hydrophobic content at each position of the surface gradient.

Here the process was demonstrated for a specific thiol; however, the proposed approach is general and can be extended to other systems able to form SAM on conductive surfaces. Future developments of this work will include the confinement of the gradient along defined structures, which could be fabricated by patterning methods such as microcontact printing,[58] lithographically controlled wetting[59] or other methods[60] and the systematic tailoring of the electrode work-function and wettability of surfaces for application in organic electronic electronics and photovoltaic.

ASSOCIATED CONTENT

Supporting Information

Description of the prototype apparatus for spatially controlled electrochemical desorption. Evolution of Cyclic voltammetry. Computer simulation: theory and system set-up. This material is available free of charge via the Internet at http://pubs.acs.org.

AUTHOR INFORMATION

Corresponding Authors

*E-mail: giulia.fioravanti@univaq.it.
*E-mail: m.cavallini@bo.ismn.cnr.it.

Author Contributions

The manuscript was written through contributions of all authors. All authors have given approval to the final version of the manuscript.

Notes

The authors declare no competing financial interest.

ACKNOWLEDGMENTS

We thank Alessandra Campana for the substrate preparation characterization and useful discussion. This work was supported by the project MIUR-PRIN prot. 2009N9N8RX.

REFERENCES

(1) Suresh, S. Graded Materials for Resistance to Contact Deformation and Damage. *Science* **2001**, *292*, 2447−2451.
(2) Chaudhury, M. K.; Whitesides, G. M. How to Make Water Run Uphill. *Science* **1992**, *256* (5063), 1539−1541.
(3) Daniel, S.; Sircar, S.; Gliem, J.; Chaudhury, M. K. Ratcheting Motion of Liquid Drops on Gradient Surfaces. *Langmuir* **2004**, *20* (10), 4085−4092.
(4) Berna, J.; Leigh, D. A.; Lubomska, M.; Mendoza, S. M.; Perez, E. M.; Rudolf, P.; Teobaldi, G.; Zerbetto, F. Macroscopic Transport by Synthetic Molecular Machines. *Nat. Mater.* **2005**, *4* (9), 704−710.
(5) Han, X. J.; Wang, L.; Wang, X. J. Fabrication of Chemical Gradient Using Space Limited Plasma Oxidation and Its Application for Droplet Motion. *Adv. Funct Mater.* **2012**, *22* (21), 4533−4538.
(6) Lugli, F.; Fioravanti, G.; Pattini, D.; Pasquali, L.; Montecchi, M.; Gentili, D.; Murgia, M.; Hemmatian, Z.; Cavallini, M.; Zerbetto, F. And Yet it Moves! Microfluidics Without Channels and Troughs. *Adv. Funct Mater.* **2013**, *23* (44), 5543−5549.
(7) Cavallini, M.; Lazzaroni, R.; Zamboni, R.; Biscarini, F.; Timpel, D.; Zerbetto, F.; Clarkson, G. J.; Leigh, D. A. Conformational Self-Recognition As the Origin of Dewetting in Bistable Molecular Surfaces. *J. Phys. Chem. B* **2001**, *105* (44), 10826−10830.
(8) Cai, K. Y.; Dong, H. D.; Chen, C.; Yang, L.; Jandt, K. D.; Deng, L. H. Inkjet Printing of Laminin Gradient to Investigate Endothelial Cellular Alignment. *Colloids Surf., B* **2009**, *72* (2), 230−235.
(9) Lee, J.; Choi, I.; Yeo, W. S. Preparation of Gradient Surfaces by Using a Simple Chemical Reaction and Investigation of Cell Adhesion on a Two-Component Gradient. *Chem.—Eur. J.* **2013**, *19* (18), 5609−5616.
(10) Elwing, H.; Welin, S.; Askendal, A.; Nilsson, U.; Lundstrom, I. A Wettability Gradient-Method for Studies of Macromolecular Interactions at the Liquid Solid Interface. *J. Colloid Interface Sci.* **1987**, *119* (1), 203−210.
(11) Albert, J. N. L.; Baney, M. J.; Stafford, C. M.; Kelly, J. Y.; Epps, T. H. Generation of Monolayer Gradients in Surface Energy and Surface Chemistry for Block Copolymer Thin Film Studies. *ACS Nano* **2009**, *3* (12), 3977−3986.

(12) Zhu, X.; Wang, H.; Liao, Q.; Ding, Y. D.; Gu, Y. B. Experiments and Analysis on Self-Motion Behaviors of Liquid Droplets on Gradient Surfaces. *Exp Therm Fluid Sci.* **2009**, *33* (6), 947−954.
(13) Zhao, H.; Law, K. Y. Super Toner and Ink Repellent Superoleophobic Surface. *Acs Appl. Mater. Inter* **2012**, *4* (8), 4288−4295.
(14) Liedberg, B.; Tengvall, P. Molecular Gradients of Omega-Substituted Alkanethiols on Gold - Preparation and Characterization. *Langmuir* **1995**, *11* (10), 3821−3827.
(15) Morgenthaler, S.; Lee, S. W.; Zurcher, S.; Spencer, N. D. A Simple, Reproducible Approach to the Preparation of Surface-Chemical Gradients. *Langmuir* **2003**, *19* (25), 10459−10462.
(16) Venkataraman, N. V.; Zurcher, S.; Spencer, N. D. Order and Composition of Methyl-Carboxyl and Methyl-Hydroxyl Surface-Chemical Gradients. *Langmuir* **2006**, *22* (9), 4184−4189.
(17) Morgenthaler, S. M.; Lee, S.; Spencer, N. D. Submicrometer Structure of Surface-Chemical Gradients Prepared by a Two-Step Immersion Method. *Langmuir* **2006**, *22* (6), 2706−2711.
(18) Choi, S. H.; Newby, B. M. Z. Micrometer-Scaled Gradient Surfaces Generated Using Contact Printing of Octadecyltrichlorosilane. *Langmuir* **2003**, *19* (18), 7427−7435.
(19) Kraus, T.; Stutz, R.; Balmer, T. E.; Schmid, H.; Malaquin, L.; Spencer, N. D.; Wolf, H. Printing Chemical Gradients. *Langmuir* **2005**, *21* (17), 7796−7804.
(20) Geissler, M.; Chalsani, P.; Cameron, N. S.; Veres, T. Patterning of Chemical Gradients with Submicrometer Resolution Using Edge-Spreading Lithography. *Small* **2006**, *2* (6), 760−765.
(21) Klauser, R.; Chen, C. H.; Huang, M. L.; Wang, S. C.; Chuang, T. J.; Zharnikov, M. Patterning and Imaging of Self-Assembled Monolayers with a Focused Soft X-ray Beam. *J. Electron Spectrosc.* **2005**, *144*, 393−396.
(22) Harris, B. P.; Metters, A. T. Generation and Characterization of Photopolymerized Polymer Brush Gradients. *Macromolecules* **2006**, *39* (8), 2764−2772.
(23) Blondiaux, N.; Zurcher, S.; Liley, M.; Spencer, N. D. Fabrication of Multiscale Surface-Chemical Gradients by Means of Photocatalytic Lithography. *Langmuir* **2007**, *23* (7), 3489−3494.
(24) Ito, Y.; Heydari, M.; Hashimoto, A.; Konno, T.; Hirasawa, A.; Hori, S.; Kurita, K.; Nakajima, A. The Movement of a Water Droplet on a Gradient Surface Prepared by Photodegradation. *Langmuir* **2007**, *23* (4), 1845−1850.
(25) Liu, C. S.; Zheng, D. M.; Zhou, J. G.; Wan, Y.; Li, Z. W. Fabrication of Surface Energy Gradients Using Self-Assembled Monolayer Surfaces Prepared by Photodegradation. *Nano-Scale and Amorphous Materials* **2011**, *688*, 102−106.
(26) Ionov, L.; Sidorenko, A.; Stamm, M.; Minko, S.; Zdyrko, B.; Klep, V.; Luzinov, I. Gradient Mixed Brushes: "Grafting To" Approach. *Macromolecules* **2004**, *37* (19), 7421−7423.
(27) Genzer, J.; Bhat, R. R. Surface-Bound Soft Matter Gradients. *Langmuir* **2008**, *24* (6), 2294−2317.
(28) Morgenthaler, S.; Zink, C.; Spencer, N. D. Surface-Chemical and -Morphological Gradients. *Soft Matter* **2008**, *4* (3), 419−434.
(29) Bain, C. D.; Evall, J.; Whitesides, G. M. Formation of Monolayers by the Coadsorption of Thiols on Gold - Variation in the Head Group, Tail Group, and Solvent. *J. Am. Chem. Soc.* **1989**, *111* (18), 7155−7164.
(30) Stranick, S. J.; Parikh, A. N.; Tao, Y. T.; Allara, D. L.; Weiss, P. S. Phase-Separation of Mixed-Composition Self-Assembled Monolayers into Nanometer-Scale Molecular Domains. *J. Phys. Chem.* **1994**, *98* (31), 7636−7646.
(31) Gallant, N. D.; Lavery, K. A.; Amis, E. J.; Becker, M. L. Universal Gradient Substrates for "Click" Biofunctionalization. *Adv. Mater.* **2007**, *19* (7), 965−+.
(32) Moumen, N.; Subramanian, R. S.; McLaughlin, J. B. Experiments on the Motion of Drops on a Horizontal Solid Surface Due to a Wettability Gradient. *Langmuir* **2006**, *22* (6), 2682−2690.
(33) Welin-Klintstrom, S.; Lestelius, M.; Liedberg, B.; Tengvall, P. Comparison between Wettability Gradients Made on Gold and on Si/SiO_2 Substrates. *Colloids Surf., B* **1999**, *15* (1), 81−87.
(34) Hakkinen, H. The Gold-Sulfur Interface at the Nanoscale. *Nat. Chem.* **2012**, *4* (6), 443−455.
(35) Love, J. C.; Estroff, L. A.; Kriebel, J. K.; Nuzzo, R. G.; Whitesides, G. M. Self-Assembled Monolayers of Thiolates on Metals As a Form of Nanotechnology. *Chem. Rev.* **2005**, *105* (4), 1103−1169.
(36) Cavallini, M.; Aloisi, G.; Bracali, M.; Guidelli, R. An in Situ STM Investigation of Uracil on Ag(111). *J. Electroanal. Chem.* **1998**, *444* (1), 75−81.
(37) Ma, F. Y.; Lennox, R. B. Potential-Assisted Deposition of Alkanethiols on Au: Controlled Preparation of Single- and Mixed-Component SAMs. *Langmuir* **2000**, *16* (15), 6188−6190.
(38) Petrovic, Z.; Metikos-Hukovic, M.; Babic, R. Potential-Assisted Assembly of 1-Dodecanethiol on Polycrystalline Gold. *J. Electroanal. Chem.* **2008**, *623* (1), 54−60.
(39) Tencer, M.; Berini, P. Toposelective Electrochemical Desorption of Thiol SAMs from Neighboring Polycrystalline Gold Surfaces. *Langmuir* **2008**, *24* (21), 12097−12101.
(40) Wong, E. H. J.; May, G. L.; Wilde, C. P. Oxidative Desorption of Thiols As a Route to Controlled Formation of Binary Self Assembled Monolayer Surfaces. *Electrochim. Acta* **2013**, *109*, 67−74.
(41) Lee, L. Y. S.; Lennox, R. B. Electrochemical Desorption of n-Alkylthiol SAMs on Polycrystalline Gold: Studies Using a Ferrocenylalkylthiol Probe. *Langmuir* **2007**, *23* (1), 292−296.
(42) Zhong, C. J.; Porter, M. D. Fine Structure in the Voltammetric Desorption Curves of Alkanethiolate Monolayers Chemisorbed at Gold. *J. Electroanal. Chem.* **1997**, *425* (1-2), 147−153.
(43) Lemay, D. M.; Shepherd, J. L. Electrochemical Fabrication of a Heterogeneous Binary SAM on Polycrystalline Au. *Electrochim. Acta* **2008**, *54* (2), 388−393.
(44) Smith, S. R.; Han, S.; McDonald, A.; Zhe, W.; Shepherd, J. L. An Electrochemical Approach to Fabricate a Heterogeneous Mixed Monolayer on Planar Polycrystalline Au and Its Characterization with Lateral Force Microscopy. *J. Electroanal. Chem.* **2012**, *666*, 76−84.
(45) Terrill, R. H.; Balss, K. M.; Zhang, Y. M.; Bohn, P. W. Dynamic Monolayer Gradients: Active Spatiotemporal Control of Alkanethiol Coatings on Thin Gold Films. *J. Am. Chem. Soc.* **2000**, *122* (5), 988−989.
(46) Balss, K. M.; Kuo, T. C.; Bohn, P. W. Direct Chemical Mapping of Electrochemically Generated Spatial Composition Gradients on Thin Gold Films with Surface-Enhanced Raman Spectroscopy. *J. Phys. Chem. B* **2003**, *107* (4), 994−1000.
(47) Baikie, I. D.; Mackenzie, S.; Estrup, P. J. Z.; Meyer, J. A. Noise and the Kelvin Method. *Rev. Sci. Instrum.* **1991**, *62* (5), 1326−1332.
(48) Kakiuchi, T.; Usui, H.; Hobara, D.; Yamamoto, M. Voltammetric Properties of the Reductive Desorption of Alkanethiol Self-Assembled Monolayers from a Metal Surface. *Langmuir* **2002**, *18* (13), 5231−5238.
(49) Sumi, T.; Uosaki, K. Electrochemical Oxidative Formation and Reductive Desorption of a Self-Assembled Monolayer of Decanethiol on a Au(111) Surface in KOH Ethanol Solution. *J. Phys. Chem. B* **2004**, *108* (20), 6422−6428.
(50) Duwez, A. S. Exploiting Electron Spectroscopies to Probe the Structure and Organization of Self-Assembled Monolayers: A Review. *J. Electron Spectrosc.* **2004**, *134* (2-3), 97−138.
(51) Liscio, A.; Palermo, V.; Samori, P. Nanoscale Quantitative Measurement of the Potential of Charged Nanostructures by Electrostatic and Kelvin Probe Force Microscopy: Unraveling Electronic Processes in Complex Materials. *Acc. Chem. Res.* **2010**, *43* (4), 541−550.
(52) Zehner, R. W.; Parsons, B. F.; Hsung, R. P.; Sita, L. R. Tuning the Work Function of Gold with Self-Assembled Monolayers Derived from X-[C_6H_4-C C-](n)C_6H_4-SH (n = 0, 1, 2; X = H, F, CH_3, CF_3, and OCH_3). *Langmuir* **1999**, *15* (4), 1121−1127.
(53) Espanol, P.; Warren, P. Statistical-Mechanics of Dissipative Particle Dynamics. *Europhys. Lett.* **1995**, *30* (4), 191−196.
(54) Groot, R. D.; Warren, P. B. Dissipative Particle Dynamics: Bridging the Gap between Atomistic and Mesoscopic Simulation. *J. Chem. Phys.* **1997**, *107* (11), 4423−4435.

(55) Lugli, F.; Brini, E.; Zerbetto, F. Shape Governs the Motion of Chemically Propelled Janus Swimmers. *J. Phys. Chem. C* **2012**, *116* (1), 592−598.
(56) Kong, B.; Yang, X. Z. Dissipative Particle Dynamics Simulation of Contact Angle Hysteresis on a Patterned Solid/Air Composite Surface. *Langmuir* **2006**, *22* (5), 2065−2073.
(57) Clark, A. T.; Lal, M.; Ruddock, J. N.; Warren, P. B. Mesoscopic Simulation of Drops in Gravitational and Shear Fields. *Langmuir* **2000**, *16* (15), 6342−6350.
(58) Xia, Y. N.; Whitesides, G. M. Soft Lithography. *Annu. Rev. Mater. Sci.* **1998**, *28*, 153−184.
(59) Cavallini, M.; Gentili, D.; Greco, P.; Valle, F.; Biscarini, F. Micro- and Nanopatterning by Lithographically Controlled Wetting. *Nat. Protoc.* **2012**, *7* (9), 1668−1676.
(60) Cavallini, M.; Gomez-Segura, J.; Albonetti, C.; Ruiz-Molina, D.; Veciana, J.; Biscarini, F. Ordered Patterning of Nanometric Rings of Single Molecule Magnets on Polymers by Lithographic Control of Demixing. *J. Phys. Chem. B* **2006**, *110* (24), 11607−11610.